

## Sound Absorption Properties of Oil Palm Fibre–Polylactic Acid-Based Micro-Perforated Panels with Compatibilizer

WMA Wan Mamat Ali<sup>1\*</sup>, Zaidi Mohd Ripin<sup>1</sup>, L. E. Ooi<sup>1</sup>, M.Z.A Thirmizir<sup>2</sup>,  
C. K. Abdullah<sup>3</sup>

<sup>1</sup>*TheVibrationLab, School of Mechanical Engineering, Universiti Sains Malaysia,*

<sup>2</sup>*Science and Engineering Research Centre, Engineering Campus, Universiti Sains Malaysia.*

<sup>3</sup>*Green BioPolymer, Coatings & Packaging Cluster, School of Industrial Technology, Universiti Sains Malaysia.*

Received 1 Jun 2025

Accepted 30 Jul 2025

### Abstract

Micro-Perforated Panels (MPP) are widely recognized for their effectiveness in passive noise control, relying on submillimetre perforations to achieve sound absorption without traditional fibrous fillers. The shift towards sustainable materials has prompted the exploration of bio-composites incorporating natural fibres for acoustic applications. Oil palm fibre (OPF), a by-product of agricultural waste, offers a renewable and biodegradable reinforcement when integrated with polylactic acid (PLA) to form Bio-Composite MPPs (BC-MPP). This study aims to investigate the acoustic and mechanical performance of BC-MPP fabricated from OPF/PLA composites with a compatibilizer. A systematic approach encompassing material fabrication, tensile testing, Scanning Electron Microscopy (SEM), and Sound Absorption Coefficient (SAC) analysis was adopted to assess the influence of fibre content and air gap variation. BC-MPP achieved a maximum SAC of 1.00 at 1530 Hz with 30% OPF and a 10 mm air gap. With increasing air gaps (20 mm and 30 mm), SAC values of 0.99 were recorded at 970 Hz and 800 Hz, respectively. Mechanical analysis showed a reduction in tensile strength at higher OPF contents, attributed to fibre pull-out and interfacial voids. This study presents an eco-friendly acoustic solution using agro-waste-derived composites. Future work will explore fibre surface treatment and hybrid reinforcement strategies to optimize both acoustic and mechanical performance.

© 2025 Jordan Journal of Mechanical and Industrial Engineering. All rights reserved

**Keywords:** Bio-composite materials, Micro-perforated panel (MPP), Acoustic absorption, Sustainable engineering materials, Mechanical systems noise control.

### 1. Introduction

The increasing demand for sustainable acoustic solutions has driven interest in micro-perforated panels (MPP), which rely on submillimetre perforations to attenuate sound via viscous and thermal dissipation mechanisms [1], [2], [3]. While traditional materials like foam and fiberglass are effective, environmental concerns and performance limitations necessitate alternatives. Natural fibre-based composites offer a biodegradable, cost-effective, and structurally adaptable option for noise control, particularly in industrial and mechanical systems [4], [5], [6], [7].

Recent advancements in acoustic engineering have introduced micro-perforated panel (MPP) systems integrated with fibrous materials to enhance sound absorption across a wide frequency spectrum [5], [6]. Natural fibres such as silk cotton, cellulose, and basalt fibre composites have demonstrated excellent acoustic damping due to their porous structure and energy dissipation capacity [8], [9], [10], [11]. The use of biocomposites in MPPs combines the benefits of natural

fibre absorption with the tunability of micro-perforations [12], [13]. Studies have also shown that polylactic acid (PLA), as a biodegradable matrix, can be reinforced with agro-waste fibres such as oil palm fibre (OPF), offering environmental benefits and functional mechanical properties [3], [14], [15], [16]. However, conventional MPPs often employ metallic substrates, such as aluminium and steel, which pose recyclability and biodegradability challenges [17]. Therefore, the integration of natural fibres in biodegradable matrices represents a shift towards more sustainable acoustic materials [18], [19], [20], [21].

Despite promising acoustic outcomes, current natural fibre-based MPPs suffer from mechanical limitations, including reduced tensile strength and fibre–matrix interfacial issues, particularly under varying structural loads [22], [23], [24]. Many studies focus on the acoustic benefits of natural fibres but overlook the need for sufficient mechanical integrity for industrial applications. Additionally, the combination of OPF and PLA often leads to poor adhesion due to their hydrophobic and hydrophilic mismatch, respectively [14], [15], [16], [25]. The lack of compatibilization strategies in existing literature leaves a gap in optimizing the composite performance.

\* Corresponding author e-mail: amri@usm.my.



Furthermore, limited research addresses the effect of air gap configuration on the sound absorption coefficient (SAC) in bio-composite MPPs, despite its crucial role in resonance tuning. These unresolved challenges highlight the need for a complete investigation that integrates material selection, structural design, and performance characterization for both acoustic and mechanical functionality.

While prior studies have explored OPF/PLA composite for acoustic applications, they have largely overlooked the role of compatibilizer in enhancing fibre-matrix adhesion, which is critical for mechanical performance. Moreover, there is limited work integrating quantitative microstructural analysis with mechanical and acoustic evaluations, especially in bio-composite MPPs. Few studies statistically compare predicted and experimental SAC values or assess the influence of air gap configurations in a systematic method.

To address these gaps, this study develops and evaluates bio-composite MPPs composed of oil palm fibre (OPF), PLA and maleic anhydride-grafted polypropylene (MAPP) as a compatibilizer. The experimental approach includes tensile testing, quantitative microstructural analysis, and sound absorption measurements across varying fibre contents and air gaps. The goal is to identify optimal formulations that balance acoustic performance and mechanical integrity for engineering applications in noise-sensitive environments.

## 2. Materials and Methods

### 2.1. Materials Synthesis and characterization

Oil palm fibre (OPF), polylactic acid (PLA), and maleic anhydride-grafted polypropylene (MAPP; OREVAC® CA100/CA100N) were selected to fabricate bio-composite micro-perforated panels (BC-MPPs). OPF was cleaned, dried at 60 °C for 24 h, and ground to 1 mm particles. PLA and MAPP pellets were also pre-dried to eliminate moisture. Material properties are summarized in **Table 1**.

**Table 1.** Material properties of OPF, PLA and compatibilizer.

Material		OPF	PLA	Compatibilizer (MAPP)
Density	(kg/cm <sup>3</sup> )	0.457	1.24	0.91
	(g/cm <sup>3</sup> )	0.000457	0.000124	0.00091
Tensile Strength (MPa)		1135.11	50	-
Melting Temperature (°C)		-	175	167

Composite preparation was conducted using a torque rheometer (POTOP RTBI-200). A mixture of 150 g PLA and 10 g MAPP was processed at 175 °C and 5 rpm for 5 min, followed by the addition of 40 g OPF at 50 rpm for 10 min. This was repeated for various OPF:PLA:MAPP ratios (**Table 2**). Sheets were compression-moulded at 175 °C using a GoTech press with a cycle of 5 min preheating, 3 min pressing at 50 tons, and 5 min cooling. Samples were stored in a desiccator for 24 h before testing.

**Table 2.** The detailed formulation of the material.

Composite Material	Specimen	OPF		PLA		Compatibilizer	
		(%)	(g)	(%)	(g)	(%)	(g)
OPF + PLA + Compatibilizer (BC)	BC-1	20	40	75	150	5	10
	BC-2	30	60	65	130	5	10
	BC-3	40	80	55	110	5	10
	BC-4	50	100	45	90	5	10
	BC-5	60	120	35	70	5	10

Tensile properties were assessed per ASTM D638 (Type IV) using an Instron 3367 at 1 mm/min under controlled conditions (23 ± 2 °C, 50% RH). Dumbbell specimens (1 mm thick, 15 mm wide, 150 mm long) were tested in triplicate. Surface and fracture morphology were observed using FE-SEM (FEI Varios 460L).

### 2.2. Theory of Micro-Perforated Panel

The acoustic impedance of a tube can be described by the following equation, as long as the wavelength of the incoming sound is longer than the tube's diameter and the spacing between the tubes.

$$Z = j\omega\rho t \left[ 1 - \left( \frac{2}{\xi\sqrt{-j}} \right) \left( \frac{J_1(\xi\sqrt{-j})}{J_0(\xi\sqrt{-j})} \right) \right]^{-1} \quad (1)$$

$$\xi = r_0 \sqrt{\rho\omega\eta} \quad (2)$$

Here  $J_0$  and  $J_1$  are quantified to as the zeroth- and first-order Bessel functions of the first type,  $\omega$  is the sound's angular frequency,  $\rho$  is the air density,  $t$  is the thickness of the plate,  $r_0$  is the perforated hole's radius, and  $\eta$  is the air dynamic viscosity,  $\xi$ . The acoustic impedance value of the MPP can be determined by dividing Eq. (1) by the ratio of the perforated area to the total surface area of the panel. Since the acoustic impedance of Eq. (1) is not practical, [26] suggested a better method with an inaccuracy of less than 5%. The normalized acoustic impedance of MPP, or  $Z_{pM}$ , is expressed as [26], [27]:

$$Z_{pM} = \left( \frac{Z}{Z_0} \right) = R_{pM} + jX_{pM}, \quad (3)$$

$$R_{pM} = \frac{c_1 t \times 10^{-5}}{pd^2} \left( \sqrt{1 + \frac{x^2}{32} + \frac{xd\sqrt{2}}{8t}} \right), \quad (4)$$

$$X_{pM} = 0.0185 \frac{tf}{p} \left( 1 + \frac{1}{\sqrt{9 + \frac{x^2}{2}}} + \frac{0.85d}{t} \right), \quad (5)$$

$$\chi = C_2 \times 10^{-3} d \sqrt{f} \quad (6)$$

Where  $C_1$  and  $C_2$  are 0.147 and 0.316 for nonmetal MPP and 0.335 and 0.21 for metal MPP,  $R_{pM}$  and  $X_{pM}$  are defined as the resistance and reactance of the MPP, respectively, while  $f$  denotes the frequency and  $d$  represents the diameter of the perforated hole. The formula below can be used to calculate the sound absorption coefficient ( $\alpha$ ) of MPP under normal incidence conditions with an air gap.

$$\alpha = \frac{4R_{pM}}{(1 + R_{pM})^2 + [\omega \times X_{pM} - \cot(\omega D/C_0)]^2} \quad (7)$$

where  $C_0$  is the sound speed at which the MPP is struck.

### 2.3. Sound Absorption Coefficient Measurement

The acoustic performance of MPPs was predicted using Maa's impedance model [26], [27], [28], [29]. The micro-perforation diameter was fixed at 0.8 mm and drilled using



a CNC milling machine (FANUC ROBODRILL  $\alpha$ -T21iFLb) with a spindle speed of 10000 rpm and feed rate of 65 mm/min. The design parameters were first simulated using MATLAB to ensure target SAC values. **Table 3** presents the geometrical and acoustic parameters for each sample. SAC measurements were conducted using a two-microphone impedance tube method, in accordance with ISO 10534-2 and ASTM E1050 standards. The setup included GRAS 46AE microphones, LMS software, and a loudspeaker generating random sound signals within a frequency range of 500–3500 Hz. Specimens were inserted into a 34.8 mm diameter impedance tube with air gaps of 10, 20, and 30 mm adjusted via a movable plunger. Microphones were calibrated before each test, and the SAC was calculated using  $\alpha = 1 - |R|^2$ , where R is the reflection coefficient obtained via transfer function H12.

### 3. Results and Discussion

#### 3.1. Sound Absorption Coefficient (SAC) of Bio-Composite Samples

The variation in sound absorption coefficient (SAC) for bio-composite (BC) samples with different oil palm fibre (OPF) compositions, under varying air gap configurations (10 mm, 20 mm, and 30 mm), is presented in **Figure 1**. An analysis of **Figure 1(a)** reveals that, for a 10 mm air gap, the SAC peak occurs between 500 Hz and 600 Hz across all OPF compositions. Among the tested samples, BC-4 (50 wt.% OPF) exhibits the highest SAC values throughout the frequency range (0–2000 Hz), indicating superior acoustic damping behavior.

A similar pattern is observed in **Figures 1(b)** and **1(c)**, corresponding to 20 mm and 30 mm air gaps, respectively. The SAC peaks remain within the 500–600 Hz range, and BC-4 consistently outperforms other compositions. Notably, BC-2 (30 wt.% OPF) and BC-5 (60 wt.% OPF) rank second and third, respectively, in terms of SAC performance. This trend implies an optimal OPF loading of 50 wt.%, beyond which the acoustic performance deteriorates, likely due to increased stiffness and reduced porosity that hinder effective sound wave dissipation [23], [30].

The effect of increasing the air gap thickness marginally shifts the SAC curves while maintaining the same trend of frequency response. Greater air gaps enhance low-frequency absorption, consistent with quarter-wavelength theory and resonance effects [31]. However, the enhancement plateaus beyond 20 mm, suggesting diminishing returns with larger air cavities under the current sample configuration.

Comparison with earlier works on natural fibre-based composites indicates comparable or superior SAC values for the OPF-based BC-4 sample, reinforcing its potential as an effective eco-acoustic material [32], [33]. Prior studies have also emphasized the role of fibre dispersion, interfacial bonding, and pore structure in tailoring acoustic absorption characteristics [34]. While current findings are promising, limitations include lack of microstructural correlation and airflow resistivity data, which should be addressed in future work to strengthen structure–property relationships.

**Table 3.** Measured BC-MPP sample parameters.

Specimen	Composite Density (g/cm <sup>3</sup> )	BC sample weight (g)	BC-MPP sample weight(g)	Sample diameter (mm)	Sample thickness (mm)	Perforated hole diameter (mm)	Perforation Ratio (%)
BC-1	1.137	1.29	1.22	34.81	1.15	0.8	1.638
BC-2	1.163	1.32	1.31	34.85	1.14	0.8	1.638
BC-3	1.178	1.35	1.31	34.86	1.13	0.8	1.638
BC-4	1.205	1.41	1.36	34.82	1.15	0.8	1.638
BC-5	1.219	1.48	1.46	34.86	1.18	0.8	1.638

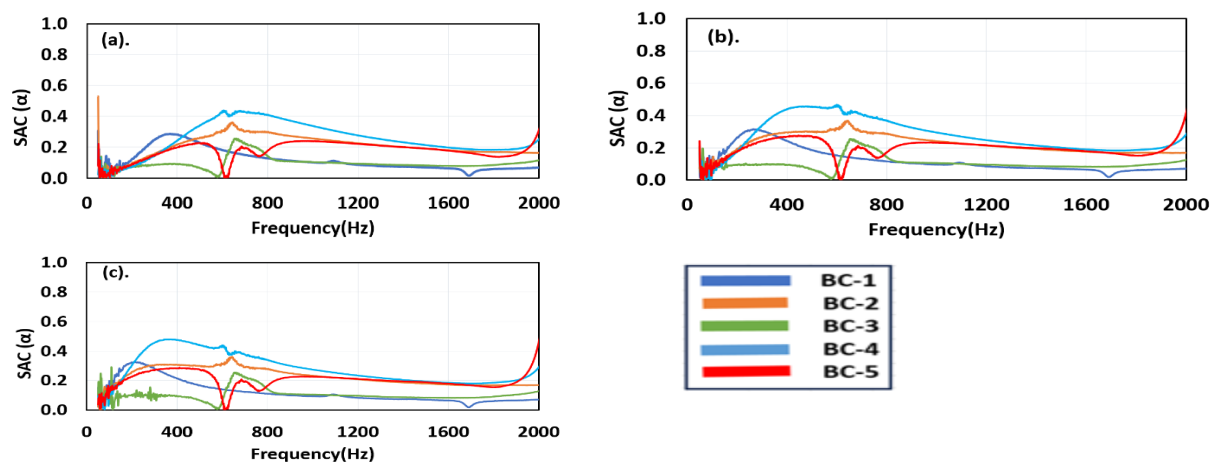


**Figure 1.** SAC for Bio-Composite (BC) samples without MPP at different OPF compositions. (a) 10 mm, (b) 20 mm, and (c) 30 mm air gap.



### 3.2. Tensile Strength of Bio-Composite

**Table 4** presents the tensile properties of bio-composite (BC) samples with varying oil palm fibre (OPF) and polylactic acid (PLA) compositions. A clear inverse relationship is observed between OPF loading and both tensile strength and elongation at break. As OPF content increases, tensile strength and ductility decline significantly. Although maleic anhydride-grafted polypropylene (MAPP) was incorporated to improve the interfacial adhesion between OPF and PLA, the reduced matrix fraction at higher OPF contents likely contributed to poor fibre wetting and dispersion. This reduction in PLA availability impedes effective stress transfer, leading to weak fibre–matrix bonding, void formation, and early failure during tensile loading [35].

**Table 4.** Tensile strength of samples with different composition percentages.

NO.	Sample	Tensile Strength (MPa)	Tensile Modulus (GPa)	Elongation at Break (%)
1	BC-1	20.43	1.55	0.85
2	BC-2	17.99	1.47	0.76
3	BC-3	16.03	1.65	0.59
4	BC-4	12.49	1.76	0.41
5	BC-5	8.42	1.60	0.31

The occurrence of fibre agglomeration becomes more pronounced at elevated OPF contents due to inadequate dispersion, further contributing to structural defects. Such voids serve as stress concentrators, accelerating crack initiation and propagation under load, thereby lowering both tensile strength and elongation [36].

In contrast, the tensile modulus increased with OPF loading up to 50% (BC-4), indicating enhanced stiffness due to the presence of rigid fibres. This increase aligns with previous studies where the incorporation of high-modulus fibres restricted matrix deformability, resulting in higher modulus values [37]. However, a slight decrease in tensile modulus at 60% OPF (BC-5) is observed, which may be attributed to matrix insufficiency, poor fibre wetting, and increased agglomeration, all of which compromise stress distribution efficiency [38].

The results highlight an optimal fibre loading threshold, specifically at 50 wt.%, that balances stiffness enhancement without severely compromising tensile strength or ductility. Beyond this point, the mechanical performance diminishes due to microstructural inhomogeneity and poor stress transfer efficiency. These findings suggest that appropriate fibre loading and processing control are essential to maximize mechanical performance in natural fibre-based composites.

### 3.3. Fractography Analysis of Tensile Fracture Surfaces

**Figure 2** presents Field Emission Scanning Electron Microscope (FESEM) micrographs of the tensile fracture surfaces of BC samples with varying OPF and PLA compositions. The analysis reveals a generally well-bonded interface between the OPF and PLA phases, with minimal interfacial gaps, particularly in samples with lower fibre content. This observation affirms the effectiveness of maleic anhydride-grafted polypropylene (MAPP) as a compatibilizer. MAPP promotes interfacial adhesion through its amphiphilic character, which enhances compatibility between the hydrophilic OPF and the hydrophobic PLA matrix [39].

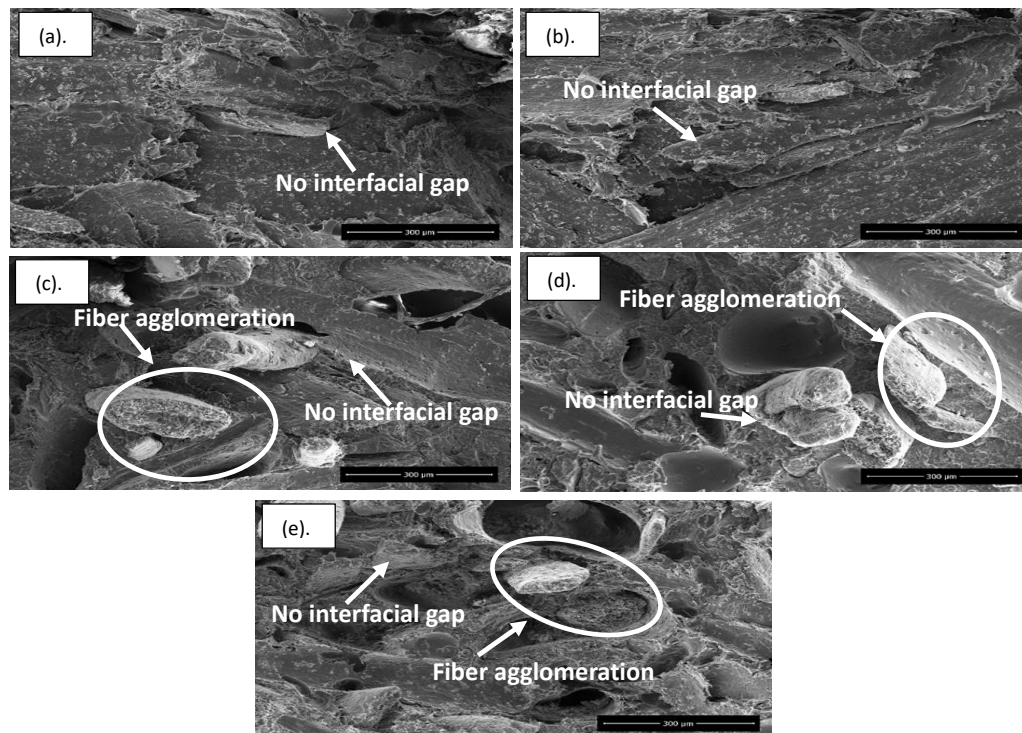


**Figure 2.** FESEM micrographs of tensile fracture surfaces of (a) CP-1, (b) CP-2, (c) CP-3, (d) CP-4, and (e) CP-5.



Nevertheless, as OPF loading increases, the micrographs reveal notable fibre agglomeration, especially in BC-3 to BC-5 samples, as indicated by circled regions in the micrographs. These agglomerated zones suggest insufficient matrix content to adequately wet and distribute the fibres. The resulting poor dispersion and inadequate matrix infiltration hinder the formation of a continuous interfacial bond, which compromises mechanical integrity.

Such morphological features correspond with the mechanical data reported in Section 3.2. The presence of agglomerates reduces the effective surface area for fibre–matrix interaction, thereby limiting stress transfer efficiency and contributing to the observed decline in tensile strength at higher OPF loadings [37]. Moreover, fibre-rich zones may promote void formation and act as crack initiation sites, further impairing the load-bearing capacity of the composite. These findings reinforce the importance of optimizing fibre loading and dispersion to achieve a balance between stiffness enhancement and structural reliability in bio-composite systems.

### 3.4. Comparison of Sound Absorption Coefficient (SAC) for BC and BC-MPP Samples

**Figure 3** compares the Sound Absorption Coefficient (SAC) of bio-composite (BC) samples with and without Micro-Perforated Panels (MPP) at varying oil palm fibre (OPF) compositions and a fixed 10 mm air gap. A significant enhancement in SAC is observed upon integration of MPP, indicating its effectiveness in improving the acoustic performance of BC materials. For instance, at 20% OPF (BC-1), the SAC increased from 0.3 at 370 Hz (without MPP) to 1.00 at 1390 Hz (with MPP). Similarly, BC-2 exhibited an increase from 0.35 at 645 Hz

to 1.00 at 1530 Hz. Notable enhancements were also recorded for BC-3 to BC-5, with peak SAC values reaching ~0.99 across the mid-to-high frequency range.

The integration of MPP shifts the peak SAC to lower frequency ranges and broadens the effective absorption bandwidth. This effect is attributed to the resonant absorption mechanism inherent to MPP structures, which complements the viscous and thermal dissipation mechanisms of porous OPF/PLA composites. These findings are consistent with prior reports by Mosa et al. [24] and Prasetyo et al. [40], which demonstrated that MPP can modify acoustic impedance and shift peak SAC values toward lower frequencies.

Across all fibre loadings, the presence of MPP enhanced SAC values, especially in the mid-frequency range (1000–1600 Hz), thus extending the acoustic absorption performance. However, it is also observed that the degree of enhancement is influenced by fibre composition. The 50% OPF composition (BC-4) consistently exhibits the highest SAC, reaffirming its optimal acoustic performance. Nevertheless, as discussed in Section 3.2, increased OPF content compromises mechanical integrity due to insufficient matrix availability and increased void content, as also evidenced by FESEM analysis.

The synergistic effect of MPP and air gaps further enhances SAC performance. Air gaps facilitate multiple reflections and extended wave paths, improving absorption particularly at higher frequencies [41]. However, gains become less pronounced beyond 20–30 mm air gap configurations.

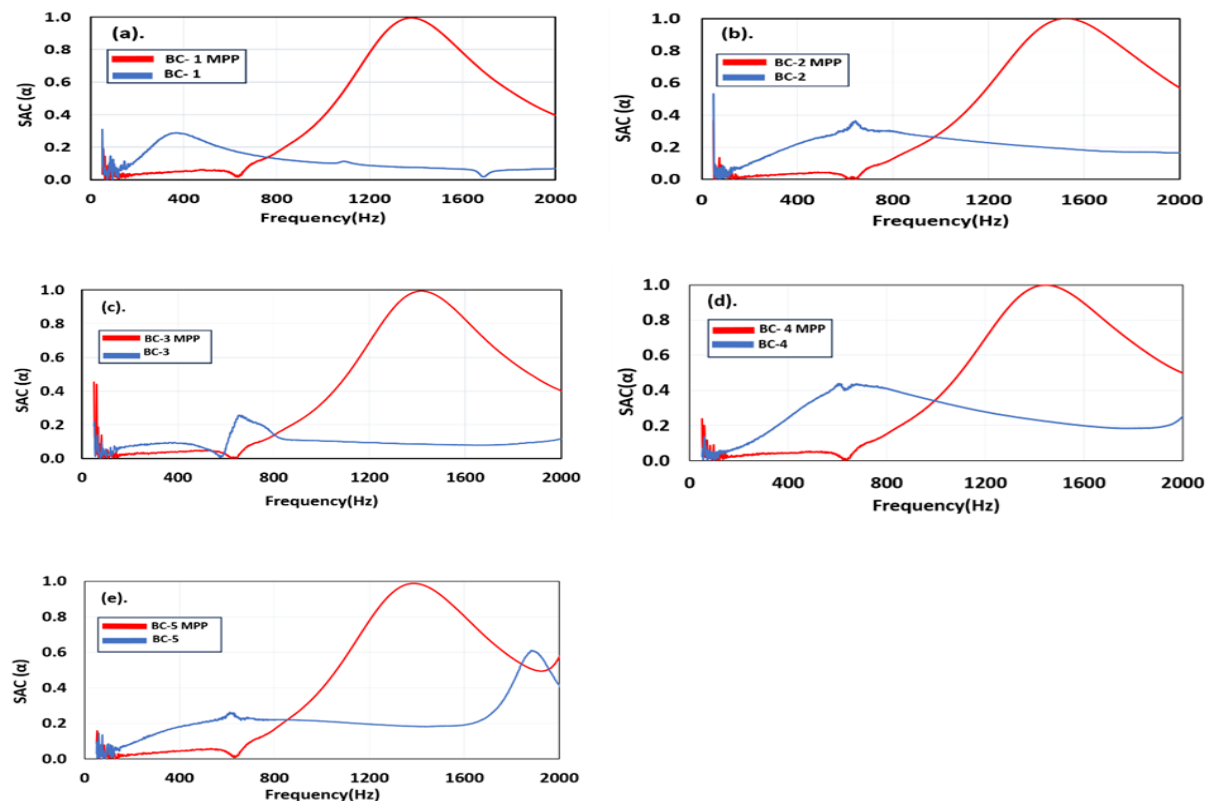


**Figure 3.** Sound absorption coefficient (SAC) of Bio-Composite Sample measured BC and BC-MPP micro-perforated panel (MPP) with an air gap of 10 mm for (a) BC-1, (b) BC-2, (c) BC-3, (d) BC-4, and (e) BC-5.



The underlying mechanisms of SAC differ significantly between porous composites and MPP. While porous layers dissipate sound via viscous drag and thermal conduction, MPPs function through resonance of trapped air masses within micro-perforations, which are tunable through geometric and material parameters [42]. The combination of both mechanisms results in a broadened and enhanced absorption profile. In contrast, BC samples without MPP lack this resonance-based absorption, leading to higher SAC peaks at relatively higher frequencies [43].

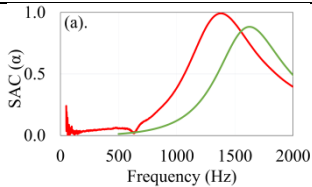
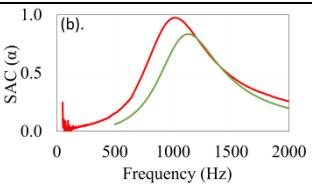
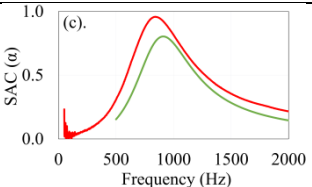
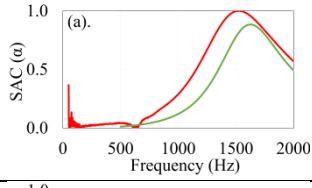
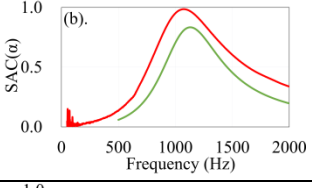
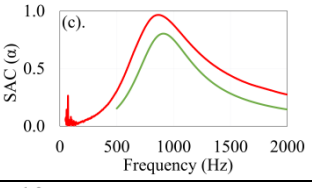
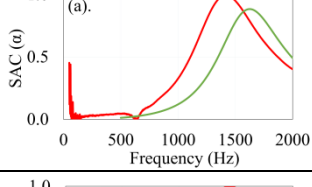
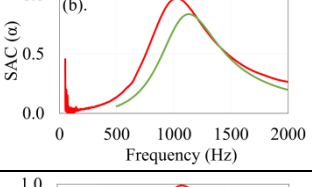
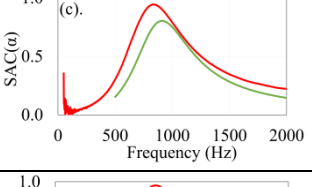
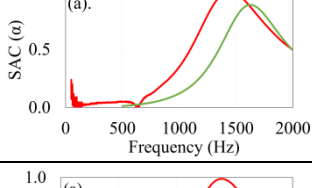
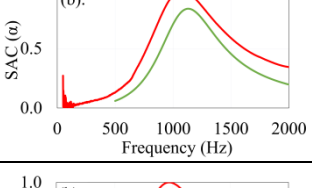
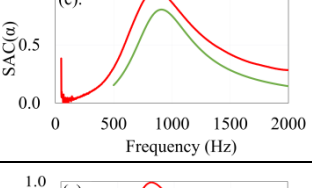
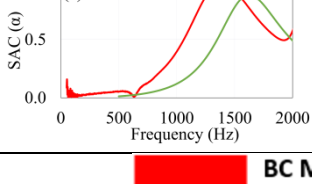
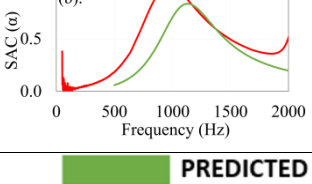
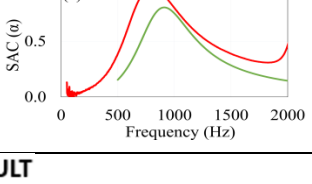


The integration of MPP with OPF/PLA bio-composites substantially improves their acoustic performance, enabling tunability of absorption characteristics through modulation of fibre loading, MPP structure, and air gap thickness. These enhancements, however, must be balanced against mechanical limitations imposed by high fibre loadings. Thus, a multi-parameter optimization approach is essential to develop bio-composites with superior sound absorption and adequate structural durability for targeted acoustic applications.

### 3.5. Comparison Between Predicted and Measured Sound Absorption Coefficients (SAC)

Table 5 presents a comparative analysis of the predicted and experimentally measured Sound Absorption Coefficient (SAC) values for bio-composite micro-perforated panels (BC-MPP) samples BC-1 to BC-5, under three different air gap configurations (10 mm, 20 mm, and 30 mm), across the frequency range of 50–2000 Hz. In all cases, the measured SAC values exceed the predicted results, and the resonance frequencies are consistently shifted to lower frequencies as the air gap increases.

For the 10 mm air gap, sample BC-1 exhibited a predicted SAC of 0.88 at 1630 Hz, while the measured value reached 0.95 at 1400 Hz. Similar improvements were observed for other samples: BC-2 (1.00 at 1530 Hz), BC-3 (0.99 at 1430 Hz), BC-4 (0.95 at 1443 Hz), and BC-5 (0.98 at 1400 Hz). The trend continued for the 20 mm air gap, where resonance frequencies further decreased. For instance, BC-1 demonstrated a predicted SAC of 0.83 at 1140 Hz, while the measured SAC increased to 0.97 at 1021 Hz. Sample BC-5 reached a measured SAC of 0.99 at 970 Hz. For the 30 mm air gap, all samples recorded resonance frequencies below 900 Hz, with BC-5 attaining 0.99 at 800 Hz.

**Table 5.** Comparison of predicted and measured SAC of BC-MPP.

SAMPLE	AIR GAP		
	10MM	20MM	30MM
BC-1	(a). 	(b). 	(c). 
BC-2	(a). 	(b). 	(c). 
BC-3	(a). 	(b). 	(c). 
BC-4	(a). 	(b). 	(c). 
BC-5	(a). 	(b). 	(c). 
 <b>BC MPP</b>  <b>PREDICTED RESULT</b>			



The consistently higher measured SAC values compared to predictions can be attributed to several factors. First, slight variations in mounting conditions and the alignment of samples within the impedance tube could introduce errors not accounted for in the theoretical model [44]. Second, eigenmode vibrations arising from the mass-spring behaviour of the MPP may enhance energy dissipation, thereby increasing the actual SAC values [45]. These vibrations, coupled with structural damping effects from the natural fibre composite, may explain the broader and more effective sound absorption range observed experimentally.

Moreover, the resonance frequency shift with increasing air gap distance confirms the theoretical expectation that larger air cavities facilitate improved low-frequency absorption by extending the effective wavelength of interacting sound waves. This phenomenon supports the practical application of air gap tuning to target specific frequency ranges.

The experimental results validate the strong acoustic performance of BC-MPP configurations, with SAC values consistently exceeding 0.90 across a broad frequency range. The findings highlight the importance of considering real-world structural interactions and panel dynamics when modeling acoustic materials. Future models should integrate complex mechanical–acoustic coupling effects to better reflect measured data and further optimize bio-composite panel designs for targeted sound absorption.

The measured SAC values exceeded the predicted values across all air gap configurations, with percentage differences ranging from 11% to 19% (**Figure 4**). The

largest differences were observed at the 30mm air gap. These differences are attributed to limitations in the theoretical model, which assumes ideal boundary conditions and uniform perforation geometry. In practise, factors such as panel edge leakage, fabrication tolerances and microphone placement introduce deviations from ideal assumptions [46]. Additionally, structural damping and complex acoustic interactions in deeper cavities may enhance the measured absorption beyond the model's scope. These findings indicate that theoretical predictions should be calibrated against experimental results, particularly for broadband absorber designs and varying air gaps [28, 46].

### 3.6. Comparison of BC-MPP at Different Air Gaps and OPF Composition Percentages

**Figure 5** illustrates the measured Sound Absorption Coefficient (SAC) of bio-composite micro-perforated panels (BC-MPP) with varying oil palm fibre (OPF), polylactic acid (PLA), and compatibilizer compositions across three air gap conditions: 10 mm, 20 mm, and 30 mm. At a 10 mm air gap, SAC values for all samples exceed 0.9, with BC-2 attaining a maximum SAC of 1.00 at 1530 Hz. The difference in SAC between samples is minimal ( $<0.02$ ), and resonance frequencies remain within a narrow range of 1400–1530 Hz, attributed to the uniform acoustic mass across samples. This observation aligns with the resonant absorber behaviour described by Bojković et al. [47], wherein MPPs reduce the natural frequency through added mass and damping.

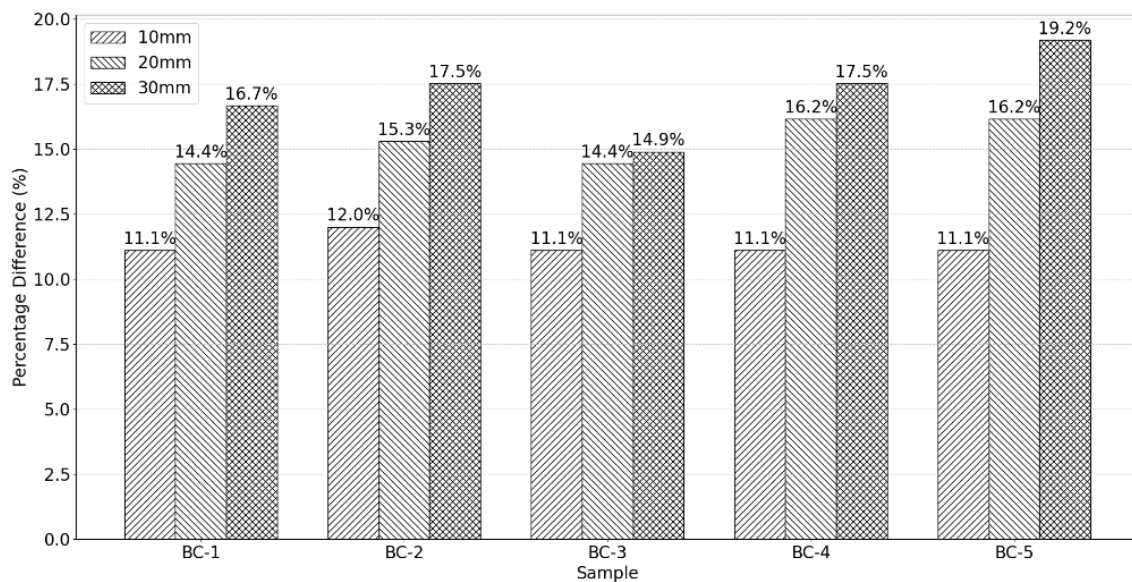


**Figure 4.** Shows the measured and predicted SAC across air gaps.



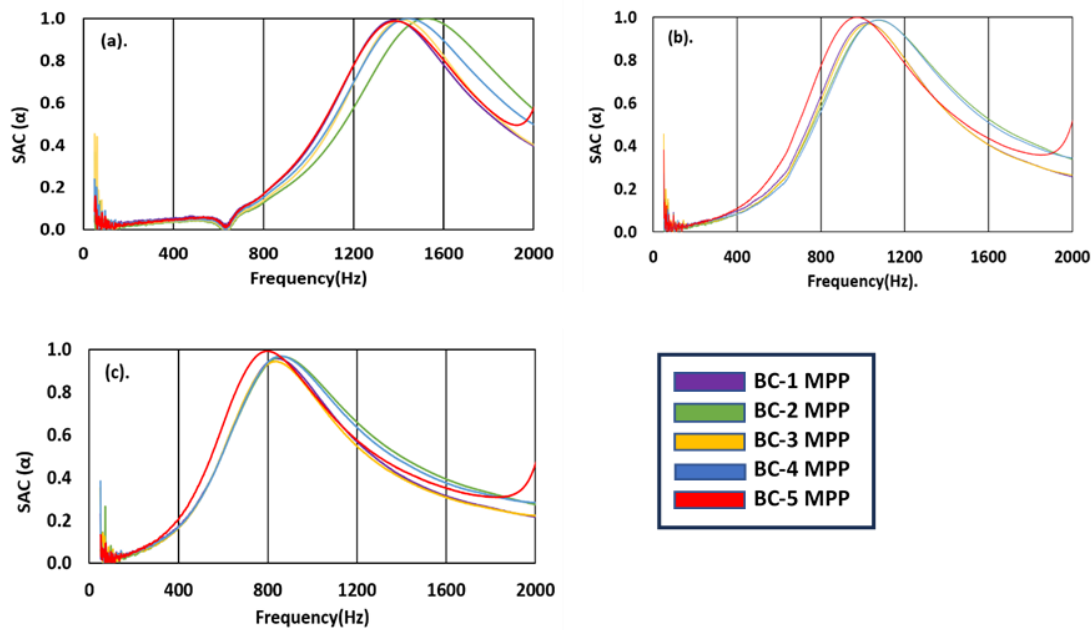


**Figure 5.** Shows the measured SAC of BC-MPP for all samples with the air gap of (a) 10 mm (b) 20 mm and (c) 30 mm.

Increasing the air gap to 20 mm results in a shift of the resonance frequencies to a lower range (973–1176 Hz), with SAC values consistently above 0.9. Notably, BC-5 achieved the highest SAC of 0.99 at 970 Hz. Further increasing the air gap to 30 mm lowers the resonance frequencies to 800–867 Hz, again with SAC values maintained around 0.9. BC-5 again demonstrated superior performance with a peak SAC of 0.99 at 800 Hz. These reductions in resonance frequency with increasing air gap are attributed to reduced system stiffness, which allows the sound waves to resonate at longer wavelengths [35], [48].

The inclusion of MPP introduces additional mass and damping, altering the system's acoustic impedance. This mass-spring interaction causes a downward shift in resonance frequency compared to non-MPP samples, which lack this mechanism [24]. Perforations in MPP act as resistive channels that increase air resistance and contribute to mass loading effects, reinforcing their role as resonant absorbers [47], [48].

Moreover, the combination of MPP with OPF-based bio-composites offers a stable and tunable acoustic profile. The downward shift in peak SAC frequencies with increasing fibre loading and air gap suggests predictable acoustic behavior, consistent with previous reports on lignocellulosic fibres [49], [50]. Natural fibres such as coconut and sugarcane have shown similar benefits in previous studies, owing to their low density, biodegradability, and micro-porous structure, which promote low-frequency absorption [51], [52].

The findings demonstrate that through careful adjustment of fibre content, MPP parameters, and air gap size, the acoustic performance of BC-MPP materials can be effectively optimized. This tunability enables targeted absorption in the low- to mid-frequency ranges, making BC-MPPs suitable for a variety of soundproofing and noise reduction applications, particularly in environmentally sustainable design contexts.

From a practical perspective, the increase in fibre loading and air gap size enhances acoustic absorption but

also contributes to greater panel thickness and weight[53]. These factors must be balanced in real-world applications, particularly where space and weight constraints exist, such as in automotive interiors and building acoustics. The optimal configuration observed in this study (30-50% OPF with 20mm air gap) offers a good compromise between sound absorption efficiency and material bulk. These findings support the potential of OPF/PLA-based MPP show high sound absorption, especially in the mid-frequency range (1000–3000 Hz), which is important for both building and automotive applications [53 - 54]. Increasing fiber content and air gap size enhances absorption, but also increases panel thickness and weight, requiring a balance for practical use.

#### 4. Conclusion

This study aims to evaluate the acoustic and mechanical performance of bio-composite micro-perforated panels (BC-MPP) developed using oil palm fibre (OPF), polylactic acid (PLA), and a compatibilizer. The objective was to investigate the influence of OPF composition, air gap thickness, and the integration of MPP on sound absorption characteristics and structural performance. Main findings are as follows:

- Maximum SAC without MPP reached 0.96 for 50% OPF (BC-4), with resonance frequencies between 500–600 Hz.
- Integration of MPP significantly increased SAC values, achieving a peak of 1.00 for BC-MPP 5 at 1530 Hz (10 mm air gap), and maintaining high SAC across 20 mm and 30 mm air gaps.
- Resonance frequency consistently shifted lower with increased air gap and MPP presence.
- Mechanical testing indicated reduced tensile strength at higher fibre loadings due to fibre agglomeration and poor matrix wetting.

This study demonstrates the potential of BC-MPPs for sustainable noise control applications. Future work should



explore dynamic damping behavior and implementation in large-scale industrial systems.

### CRediT authorship contribution statement

**WMA Wan Mamat Ali:** Supervision, Methodology, Writing – original draft. **Zaidi Mohd Ripin:** Supervision. **L. E. Ooi:** Supervision, Methodology, Writing – review and editing. **M.Z.A Thirmizir:** Resources. **C. K. Abdullah:** Resources.

### Declaration of competing interest

The authors declare that they have no known competing financial interests or personal relationships that could have appeared to influence the work reported in this paper. The authors declare that they used AI-assisted tools to check and improve the grammar, sentence structure, and overall clarity of the manuscript, to ensure it meets the journal's standards for language quality.

### Acknowledgement

The author would like to thank Universiti Sains Malaysia (USM) for sponsoring this effort through Short-Term Grant 304/PMEKANIK/6315653. The author would like to thank Universiti Sains Malaysia for providing the resources and workspace needed for this research. The author also appreciates the assistance and guidance provided by the technical staff and lecturers at Universiti Sains Malaysia.

### References

- [1] N. Nasirzadeh, Z. Beigzadeh, S. Salari, and others, 'Estimation of sound absorption behavior of combined panels comprising kenaf fibers and micro-perforated plates below 2500 Hertz', *J. Acoust. Eng.*, 2023, [Online]. Available: <https://www.researchgate.net/publication/367176236>
- [2] X. L. Gai, T. Xing, X. H. Li, and others, 'Sound absorption properties of microperforated panel with membrane cell and mass blocks composite structure', *Appl. Acoust.*, vol. 137, pp. 98–107, 2018, doi: 10.1016/j.apacoust.2018.03.013.
- [3] X. Yang, Z. Zhang, D. Wang, and others, 'Optimal design and experimental validation of sound absorbing multilayer microperforated panel with constraint conditions', *Appl. Acoust.*, vol. 146, pp. 334–344, 2019, doi: 10.1016/j.apacoust.2018.11.032.
- [4] C. Gaulon, F. Hild, J. Gérard, and others, 'Acoustic absorption of solid foams with thin membranes', *Appl. Phys. Lett.*, vol. 112, no. 26, 2018, doi: 10.1063/1.5025407.
- [5] D. Chang, B. Liu, and J. Tian, 'Improving sound absorption bandwidth of micro-perforated panel by adding porous materials', *Inter Noise J.*, 2014.
- [6] J. Carbajo, J. Ramis, L. Godinho, and others, 'Perforated panel absorbers with micro-perforated partitions', *Appl. Acoust.*, vol. 149, pp. 108–113, 2019, doi: 10.1016/j.apacoust.2019.01.023.
- [7] M. Rusli, R. S. Nanda, H. Dahlan, and others, 'Sound absorption characteristics of sandwich panel made from double leaf micro-perforated panel and natural fiber', in *IOP Conference Series: Materials Science and Engineering*, 2020, p. 012011. doi: 10.1088/1757-899X/815/1/012011.
- [8] M. L. Hackett, 'Investigating the sound absorption properties of silk cotton and other sound-absorbent materials', *Int. J. Innov. Sci. Res. Technol.*, vol. 9, no. 8, pp. 2789–2823, 2024, doi: 10.38124/ijisrt/IJISRT24AUG1664.
- [9] B. A. Sentyakov and A. A. Silin, 'The study of sound-insulating properties of fibrous materials', *J. Occup. Saf. Ind.*, vol. 8, pp. 18–22, 2024, doi: 10.24000/0409-2961-2024-8-18-22.
- [10] J. Lefebvre, B. Genestie, and A. Leblanc, 'Cellulose-based acoustic absorber with macro-controlled properties', *J. Mater. Sci. Eng.*, 2024, doi: 10.20944/preprints202409.2277.v1.
- [11] T. Yang, M. Maeder, and S. Marburg, 'Optimal design of fibrous materials for sound absorption', *J. Acoust. Soc. Am.*, vol. 154, p. A295, 2023, doi: 10.1121/10.0023575.
- [12] X. Tang and X. Yan, 'Acoustic energy absorption properties of fibrous materials: A review', *Compos. Part Appl. Sci. Manuf.*, vol. 101, pp. 360–380, 2017, doi: 10.1016/j.compositesa.2017.07.002.
- [13] G. K. Oral, A. K. Yener, and N. T. Bayazit, 'Building envelope design with the objective to ensure thermal, visual and acoustic comfort conditions', *Build. Environ.*, vol. 39, no. 3, pp. 281–287, 2004, doi: 10.1016/S0360-1323(03)00141-0.
- [14] M. Dobrzynska-Mizera, M. Dutkiewicz, T. Sterzynski, and others, 'Interfacial enhancement of polypropylene composites modified with sorbitol derivatives and siloxane-silsesquioxane resin', in *AIP Conference Proceedings*, 2015, doi: 10.1063/1.4937327.
- [15] R. Watanabe, A. Sugahara, H. Hagihara, and others, 'Insight into interfacial compatibilization of glass-fiber-reinforced polypropylene (PP) using maleic-anhydride modified PP employing infrared spectroscopic imaging', *Compos. Sci. Technol.*, vol. 199, 2020, doi: 10.1016/j.compscitech.2020.108379.
- [16] X. Zhang, F. Zhang, W. Zhang, and others, 'Enhance the interaction between ammonium polyphosphate and epoxy resin matrix through hydrophobic modification with cationic latex', *Colloids Surf. Physicochem. Eng. Asp.*, vol. 610, 2021, doi: 10.1016/j.colsurfa.2020.125917.
- [17] D. Herrin, J. Liu, and A. Seybert, 'Properties and applications of microperforated panels', 2011.
- [18] R. Fernea, D. R. Tămaş-Gavrea, D. L. Manea, and others, 'Multicriterial analysis of several acoustic absorption building materials based on hemp', *Procedia Eng.*, pp. 1005–1012, 2017, doi: 10.1016/j.proeng.2017.02.500.
- [19] C. Othmani, M. Chouireb, H. Hammami, and others, 'Experimental and theoretical investigation of the acoustic performance of sugarcane wastes based material', *Appl. Acoust.*, vol. 109, pp. 90–96, 2016, doi: 10.1016/j.apacoust.2016.02.005.
- [20] E. Taban, A. Khavanin, M. Faridan, and others, 'Comparison of acoustic absorption characteristics of coir and date palm fibers: Experimental and analytical study of green composites', *Environ. Sci. Pollut. Res.*, vol. 17, no. 1, pp. 39–48, 2020, doi: 10.1007/s13762-019-02304-8.
- [21] A. E. Tiuc, O. Nemeş, H. Vermeşan, and others, 'New sound absorbent composite materials based on sawdust and polyurethane foam', *Compos. Part B Eng.*, vol. 165, pp. 120–130, 2019, doi: 10.1016/j.compositesb.2018.11.103.
- [22] D. D. V. S. Chin, M. N. Bin Yahya, N. Bin Che Din, and others, 'Acoustic properties of biodegradable composite micro-perforated panel (BC-MPP) made from kenaf fibre and polylactic acid (PLA)', *Appl. Acoust.*, vol. 138, pp. 179–187, 2018, doi: 10.1016/j.apacoust.2018.04.009.
- [23] R. Zulkifli, M. J. M. Nor, M. Z. Nuawi, and others, 'Acoustic properties of multilayer coir fibres sound absorption panels', *Appl. Acoust.*, vol. 71, no. 2, pp. 241–246, 2010.
- [24] A. I. Mosa, A. Putra, R. Ramlan, and others, 'Wideband sound absorption of a double-layer microperforated panel with inhomogeneous perforation', *Appl. Acoust.*, vol. 161, 2020, doi: 10.1016/j.apacoust.2019.107167.



- [25] C. Wu, X. Wang, J. Zhang, and others, 'Microencapsulation and surface functionalization of ammonium polyphosphate via in-situ polymerization and thiol-ene photogated reaction for application in flame-retardant natural rubber', *Ind. Eng. Chem. Res.*, vol. 58, no. 37, pp. 17346–17358, 2019, doi: 10.1021/acs.iecr.9b02464.
- [26] D. Y. Maa, 'Theory and design of microperforated panel sound-absorbing constructions', *J. Acoust. Sci.*, 1975, [Online]. Available: <https://api.semanticscholar.org/CorpusID:115008933>
- [27] D. Y. Maa, 'Direct and accurate measurements of acoustical impedance of the microperforated panel', *J. Acoust. Sci.*, 1983, [Online]. Available: <https://api.semanticscholar.org/CorpusID:112453475>
- [28] D.-Y. Maa, 'Potential of microperforated panel absorber', *J. Acoust. Soc. Am.*, vol. 104, no. 5, 1998, doi: 10.1121/1.423870.
- [29] M. Toyoda, R. L. Mu, and D. Takahashi, 'Relationship between Helmholtz-resonance absorption and panel-type absorption in finite flexible microperforated-panel absorbers', *Appl. Acoust.*, vol. 71, no. 4, pp. 315–320, 2010, doi: 10.1016/j.apacoust.2009.10.007.
- [30] F. Asdrubali, F. D'Alessandro, and S. Schiavoni, 'A review of sustainable materials for acoustic applications', *Build. Acoust.*, vol. 22, no. 1, pp. 1–24, 2015.
- [31] J. Kang and M. Brocklesby, 'Feasibility of applying micro-perforated absorbers in acoustic design using computational simulation', *Build. Environ.*, vol. 40, no. 1, pp. 23–31, 2005.
- [32] E. Jayamani, S. Hamdan, M. E. Rahman, and others, 'Acoustic and thermal properties of natural fibre composites', *J. Eng. Sci. Technol.*, vol. 10, no. 1, pp. 43–57, 2015.
- [33] A. Putra, M. J. M. Nor, R. Zulkifli, and others, 'Using compressed coconut coir fiber as an acoustic absorber', *Appl. Acoust.*, vol. 74, no. 1, pp. 132–135, 2013.
- [34] J. P. Arenas and M. J. Crocker, 'Recent trends in porous sound-absorbing materials', *Sound Vib.*, vol. 44, no. 7, pp. 12–17, 2010.
- [35] Z. Liu, J. Zhan, M. Fard, and others, 'Acoustic properties of multilayer sound absorbers with a 3D printed micro-perforated panel', *Appl. Acoust.*, vol. 121, pp. 25–32, 2017, doi: 10.1016/j.apacoust.2017.01.032.
- [36] X. Yan, 'Void content of PP/CF wet-laid nonwoven composites: Effect of fiber content and molding conditions, and void elimination mechanism', *J. Mater. Sci.*, 2023, doi: 10.21203/rs.3.rs-2767106/v1.
- [37] N. I. Ismail and Z. A. M. Ishak, 'Effect of fiber loading on mechanical and water absorption capacity of polylactic acid/polyhydroxybutyrate-co-hydroxyhexanoate/kenaf composite', in *IOP Conference Series: Materials Science and Engineering*, 2018, p. 012014. doi: 10.1088/1757-899X/368/1/012014.
- [38] E. Ferede and D. Atalie, 'Mechanical and water absorption characteristics of sisal fiber reinforced polypropylene composite', *J. Nat. Fibers*, vol. 19, no. 16, pp. 14825–14838, 2022, doi: 10.1080/15440478.2022.2069188.
- [39] M. H. M. Hamdan, J. P. Siregar, M. R. M. Rejab, and others, 'Effect of maleated anhydride on mechanical properties of rice husk filler reinforced PLA matrix polymer composite', *Precis. Eng. Manuf.-Green Technol.*, vol. 6, no. 1, pp. 113–124, 2019, doi: 10.1007/s40684-019-00017-4.
- [40] I. Prasetyo, I. Sihar, and A. S. Sudarsono, 'Sound absorption characteristics of thin parallel microperforated panel (MPP) for random incidence field', *Appl. Acoust.*, vol. 201, 2022, doi: 10.1016/j.apacoust.2022.109131.
- [41] Y. Li, Y. Yan, and Y. Peng, 'Ultra-broadband sound absorption of a multiple-cavity metastructure with gradient thickness', *Aerosp. Sci. Technol.*, vol. 133, 2023, doi: 10.1016/j.ast.2023.108140.
- [42] W. Y. Yeang, D. Halim, X. Yi, and others, 'On improving low-frequency sound absorption using a compound microperforated panel backed by a panel-type resonator with tuned multi-frequency resonators', *J. Sound Vib.*, vol. 570, p. 118134, 2024, doi: 10.1016/j.jsv.2023.118134.
- [43] M. D. Stanciu, I. Curtu, C. Cosereanu, and others, 'Evaluation of absorption coefficient of biodegradable composite materials with textile inserts', *J. Mater. Sci.*, 2011, [Online]. Available: <https://www.researchgate.net/publication/263363795>
- [44] K. V. Horoshenkov, S. Turo, L. Pellicer, and others, 'Reproducibility experiments on measuring acoustical properties of rigid-frame porous media (round-robin tests)', *J. Acoust. Soc. Am.*, vol. 122, no. 1, pp. 345–353, 2007, doi: 10.1121/1.2739806.
- [45] K. M. Ho, Z. Yang, X. X. Zhang, and others, 'Measurements of sound transmission through panels of locally resonant materials between impedance tubes', *Appl. Acoust.*, vol. 66, no. 7, pp. 751–765, 2005, doi: 10.1016/j.apacoust.2004.11.005.
- [46] Y. Loganathan, J. S. Jeyanthi, L. Mailan Chinnapandi, and J. Pitchaimani, 'Experimental and numerical investigation on sound absorption characteristics of 3D printed coupled-cavity integrated passive element systems', *J. Low Freq. Noise Vib. Active Control*, vol. 41, pp. 146134842110421, 2022, doi: 10.1177/14613484211042157.
- [47] J. Bojkovi?, M. Maraševi?, N. Stoji?, and others, 'Thermal and sound characterization of a new biocomposite material', *Materials*, vol. 16, no. 12, 2023, doi: 10.3390/ma16124209.
- [48] B. M. Fahad and R. S. Al-Jadiri, 'Acoustic impedance evaluation of the polymer-polymer hybrid composites as insulator building materials', *Mater. Sci.*, 2023, doi: 10.20944/preprints202305.1859.v1.
- [49] M. A. Pop, C. Croitoru, S. Matei, and others, 'Thermal and sound insulation properties of organic biocomposite mixtures', *Polym. Basel*, vol. 16, no. 5, 2024, doi: 10.3390/polym16050672.
- [50] E. Tholkappiyan, D. Saravanan, R. Jagasthitha, and others, 'Prediction of acoustic performance of banana fiber-reinforced recycled paper pulp composites', *Ind. Text.*, vol. 45, no. 6, pp. 1350–1363, 2016, doi: 10.1177/1528083714559569.
- [51] E. Jayamani, S. Hamdan, S. Kok Heng, and others, 'Acoustical, thermal, and morphological properties of zein reinforced oil palm empty fruit bunch fiber biocomposites', *Appl. Polym. Sci.*, vol. 133, no. 43, 2016, doi: 10.1002/app.44164.
- [52] Y. Saygili, G. Genc, K. Y. Sanliturk, and others, 'Investigation of the acoustic and mechanical properties of homogeneous and hybrid jute and luffa bio composites', *J. Nat. Fibers*, vol. 19, no. 4, pp. 1217–1225, 2022, doi: 10.1080/15440478.2020.1764446.
- [53] V. Sekar, S. Y. E. Noum, A. Putra, S. Sivanesan, K. C. Chin, Y. S. Wong, and D. H. Kassim, 'Acoustic properties of micro-perforated panels made from oil palm empty fruit bunch fiber reinforced polylactic acid', *Sound and Vibration*, vol. 55, no. 4, pp. 343–352, 2021, doi: 10.32604/sv.2021.014916.
- [54] S. N. Nair and A. Dasari, 'Development and characterization of natural-fiber-based composite panels', *Polymers (Basel)*, vol. 14, no. 10, May 2022, doi: 10.3390/polym14102079.